Morphology Profiles Generated by Temperature Gradient in PMMA Modified Epoxy System

P. M. STEFANI *and* C. C. RICCARDI*

Institute of Materials Science and Technology (INTEMA)
University of Mar del Plata and National Research Council (CONICET)
Av. J. B. Justo 4302, 7600 Mar del Plata, Argentina

P. M. REMIRO

Dpto. Ciencia y Tecnología de Polímeros, Facultad de Ciencias Químicas
Universidad del País Vasco/Euskal Herriko Unibertsitatea
P° Manuel de Lardizábal n°3, 20009 San Sebastián/Donostia, Spain

I. MONDRAGÓN

Dpto. Ingeniería Química y Medio Ambiente
Escuela Ingeniería Técnica Industrial
Universidad del País
Vasco/Euskal Herriko Unibertsitatea
Av. Felipe IV 1-B, 20011 San Sebastián/Donostia, Spain

A diglycidyl ether of bisphenol-A (DGEBA) epoxy resin was modified with 15 wt% of poly(methylmethacrylate) (PMMA) and cured with a stoichiometric amount of 4,4'-diamino diphenyl methane (DDM). The reactive mixture was cured in a heated mold with different gradients of temperature. Temperature profiles in the mold were imposed by generation of a heat flux from the base, supported on a hot plate, and the top, cooled with water; they were measured along the mold. Depending on the thermal history in each position of the mold, the competition between the phase-separation process and reaction kinetics produces opaque or transparent zones. Phase separation can also occur in the postcure process while the gelation does not take place before. Therefore, a thermoset plate with gradient of morphology and properties was obtained. Mass fractions of PMMA dissolved in the matrix were calculated with the Fox equation from glass transition temperatures measured along the mold. They were related to morphologies developed during curing. The superposition of the phase diagrams with the conversion-temperature trajectories during cure permitted an explanation of the morphology gradients generated.

INTRODUCTION

Desirable properties of cured epoxy resins such as high modulus, creep resistance and good elevated temperature properties are counterbalanced by the fact that the unmodified matrices are often brittle and show poor resistance to crack propagation. A common method to toughen a thermoset resin is to dissolve a modifier that becomes phase separated in the course of the polymerization. Rubber modification of thermosetting polymers is extensively used for toughening these matrices (1–5). Thermoplastic-toughened epoxies have been studied as an alternative for improving fracture behavior without sacrificing other useful properties such as glass transition temperature and stiffness (6–13). As the polymerization proceeds, there is an increase in the concentration and size of the dispersed-phase particles. When the matrix reaches gelation, this separation is almost finished, but a secondary phase separation may continue inside the dispersed-phase particles (13, 14).

*Corresponding author.

The competition between phase separation and chemical reactions during the cure of modified thermosets allows us to obtain materials with several morphology profiles and therefore with different properties (15). "Sandwich" structures consisting of separated phase surface layers (opaque) and an homogeneous core (transparent) were obtained when epoxy resins were modified with castor-oil. This system shows an upper-critical solution behavior (UCST) when different cure cycles are applied (16). A phase inverted "sandwich" structure may be generated when using modifiers showing a lower-critical solution temperature behavior (LCST) (17). Also, modified cyanate ester resins, with morphology profiles, were obtained when they were cured in an oven with temperature profiles (18). More recently, phase separation of a thermoplastic polymer mixture driven by a gradient of light intensity was reported (19).

Our previous studies on the modification of epoxy resins with polymethylmethacrylate (PMMA) (20–22) show that this LCST modifier can show different morphologies in the cured mixtures by modifying only molding parameters such as temperature and precuring time.

The aim of this paper is to obtain materials with morphology profiles driven by temperature profiles in a heated mold, and to explain the resulting non-uniform aspect of cured samples arising from the competition between kinetic and phase separation processes.

EXPERIMENTAL

Materials

The epoxy resin used was DER-332, a diglycidylether of bisphenol-A, kindly supplied by Dow Chemical. It has an epoxy equivalent weight of about 175 and an hydroxyl/epoxy group ratio close to 0.015. The curing agent was 4,4'-diaminodiphenyl methane (DDM, HT-972, kindly supplied by Ciba Geigy). The PMMA (Altuglas GR 9E, Elf Atochem) had a Mn = 58,000 as measured by gel permeation chromatography in a Waters 150-C ALC/GPC instrument equipped with three columns PLGel of 500, 10^4 and 10^6 A, from Polymer Labs.

Preparation of Samples

The thermoplastic-modified epoxy mixtures were prepared in the following way: first, a weighed amount of PMMA was dissolved in dichloromethane to give an approximately 10 wt% solution. DER-332 was then added to the solution and stirred until complete dissolution of the resin. The solvent was afterwards removed by heating at 80°C in vacuum; then DDM, in a stoichiometric amine/epoxy ratio, was added and dissolved by continuously stirring the mixture for 5 min. The final amount of PMMA in the DGEBA-DDM epoxy matrix was 15 wt%. At this stage, the blend solution was transparent, thus indicating complete miscibililty.

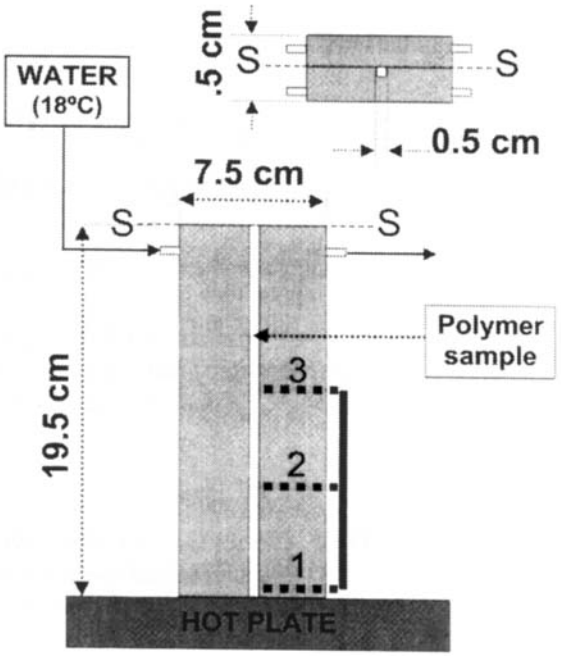

Fig. 1. Upper and lateral views of the heated mold: thermocouples positions are marked with numbers.

The curing process was performed in the heated mold shown in *Fig. 1*, for six hours. Temperature profiles were applied to the metallic mold by the generation of a heat flux from the base, supported on a hot plate, to the top, cooled with water circulating inside at a constant temperature of 18°C. Initially, the mold and the sample were at room temperature. Three profiles (A, B and C) were generated by increasing the electrical power applied to the hot plate. Temperature along the mold wall was measured with alumel-chromel thermocouples installed inside it, very close to the metal-polymer interface and connected to a multiple-channel registration device. Postcure was achieved inside an oven at 160°C for three hours.

Characterization Techniques

The glass transition temperature (Tg) profile was measured in a differential scanning calorimeter (Shimadzu DSC 50) at a heating rate of 10°C/min. Tg was taken as the onset point of the transition in the second scan.

The generated morphology profile was studied by microscopy. Cryogenic fracture surfaces were observed in tapping mode in an atomic force microscope (AFM, Nanoscope IIIa, from Digital Instruments); the topology and phase image were recorded in each sample. Transmission electron micrographs (TEM) were obtained in a Jeol JSM 35 CF microscope from specimens that had been stained with osmium tetroxide and microtomed at room temperature. All micrographs correspond to square samples having a length of 2 μm.

RESULTS AND DISCUSSION

Figure 2 is a photograph of postcured samples for each profile (A, B and C). As it was taken with light transmitted through samples, opaqueness and transparence correspond to heterogeneous and homogeneous zones, respectively.

Figure 3 shows experimental temperature-time profiles at the three-thermocouple positions shown in *Fig. 1*. Stationary temperatures of the hot plate for each profile A, B and Care 115, 155 and 206°C respectively. An energy balance considering unidirectional flux heat through the wall and the reaction term allowed us to predict conversion-temperature trajectories for each thermocouple position (see *Fig. 1*):

$$\frac{dT}{dt} = \alpha \frac{d^2T}{dz^2} + \frac{\Delta H_r}{c_P} \frac{dx}{dt} \qquad (1)$$

This equation relates conversion (x) and temperature (T) as function of time (t) and the mold thickness (z) for given constant values of thermal diffusivity (α), reaction heat (ΔH_r) and heat capacity (c_P). The validity of the unidirectional model proposed depends on two factors: first there is no polymer migration induced by the temperature gradient (23) and second, there is no significant heat flux in the axial direction. In order to check these assumptions, a sample was obtained by putting DuPont Teflon separators along the mold, before introducing the polymer sample, and by applying profile B. Neither the experimental temperature-time profiles nor the morphology profile showed detectable differences. It is worth nothing that although thermal properties vary with T and x, they were taken as constants as was reported previously (24). Experimental results for similar materials shown in the literature

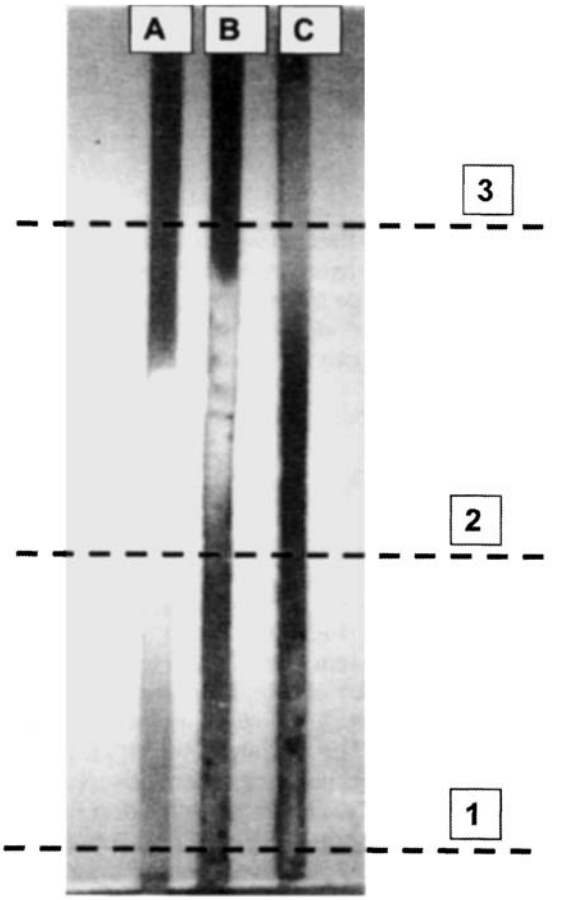

Fig. 2. Photograph of postcure samples for each profile (A, B and C). Opaqueness and transparency correspond to heterogeneous and homogeneous zones, respectively. Numbers 1, 2 and 3 correspond to thermocouple positions.

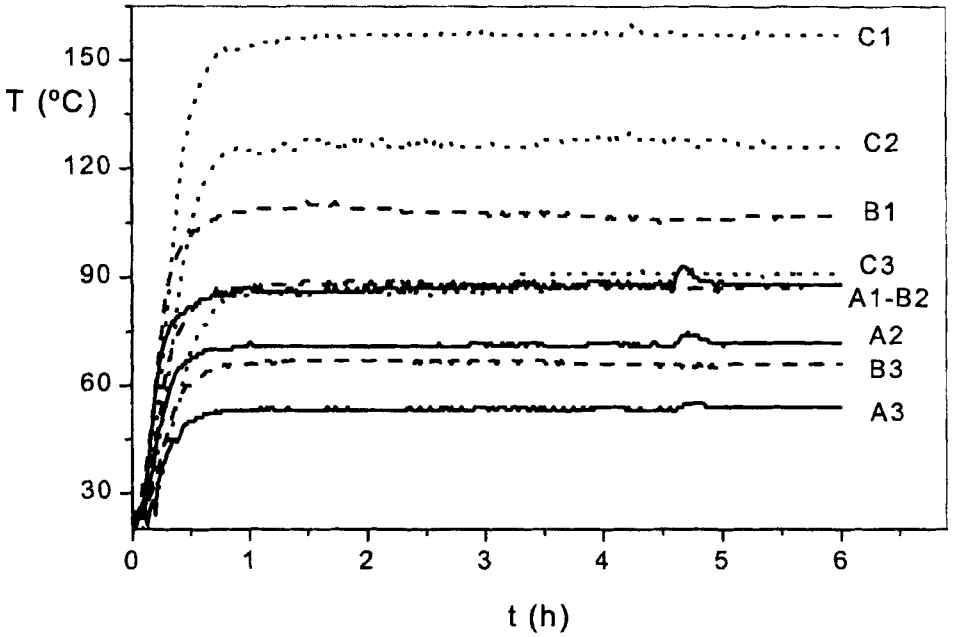

Fig. 3. Experimental temperature-time curves for each temperature gradient (A, B and C) at the three-thermocouple positions (1, 2 and 3).

Table 1. Physical Properties.

ΔH_r^{21} [KJ/Kg]	α^{24} [m²/s]	c_p^{21} [KJ/Kg K]
382.3	8.2×10^{-8}	1.94

(25, 26) established that cp values increased with temperature and decreased with conversion and that α values did not change more than 25% from the middle value. The kinetic model was the subject of previous studies (21). These physical parameters are shown in *Table 1*.

The boundary conditions are:

$$\left.\frac{dT}{dz}\right|_{z=0} = 0 \quad and \quad T|_{z=L/2} = T_w \tag{2}$$

where T_w is the experimental wall temperature and L is the sample thickness. Differential equations were solved using an explicit method of finite differences by dividing the sample thickness in ten parts and resolving the equation system each 0.3 second.

The x-T trajectories obtained during the cure process, superimposed with the cloud-point curve and the gel conversion data, previously determined (21), allow us to explain the morphology gradient observed in postcure samples (see *Fig. 2*). Phase separation takes place at temperatures higher than 91.5°C if this process is not arrested earlier by gelation. Postcured samples will be phase separated if x-T trajectory cuts the cloud-point curve before gelation or if x-T trajectories finish at conversions lower than the corresponding gel point. In this last case, phase separation occurs in the postcuring process.

Figure 4 shows the x-T curves corresponding to the mold center for each temperature profile (A, B and C). For profile A (*Fig. 4a*), it is possible to notice that for the sample at position 1, the x-T trajectory cuts the cloud-point curve very close to the gel point so final appearance is translucent. At position 2, the sample is transparent because the system gels during cure and thus the phase separation cannot occur. At position 3, the cure stops at a conversion level lower to gel point and to the corresponding cloud-point, then the sample will be phase separated during postcure, taking an opaque appearance. Similar analysis explains the morphology profiles obtained with profiles B (*Fig. 4b*) and C (*Fig. 4c*).

The mass fraction of PMMA dissolved in the matrix, ω^c_{PMMA}, was calculated with the Fox equation (27) despite other factors, like lower crosslinking density, that can depress the matrix *Tg* (20):

$$\frac{1}{Tg} = \frac{1 - \omega^c_{PMMA}}{Tg_{MATRIX}} + \frac{\omega^c_{PMMA}}{Tg_{PMMA}} \tag{3}$$

where *Tg* of the pure matrix is Tg_{MATRIX} = 165°C and the *Tg* of the thermoplastic is Tg_{PMMA} = 104°C. In *Fig. 5*, results are shown as a function of the position along the mold, for each temperature profile. Each thermocouple position is marked with numbers 1, 2 and 3. Open symbols correspond to transparent sections, dot center symbols correspond to translucent sections and the corresponding opaque sections

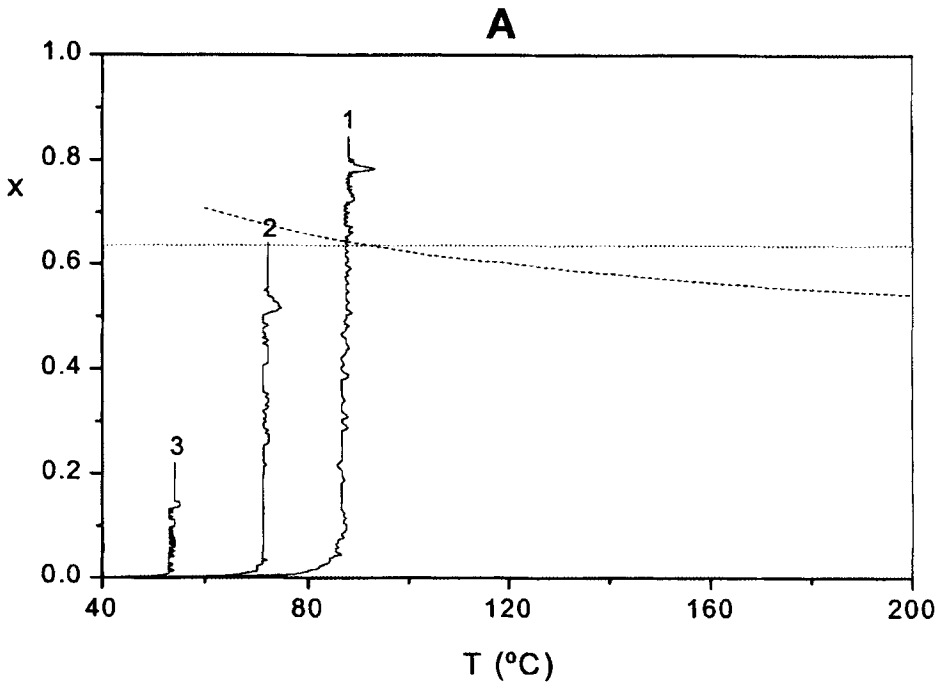

Fig. 4. x-T trajectories corresponding to the mold center (——), and cloud-point (– –) and gelation curves (·····); a) A profile, b) B profile and c) C profile.

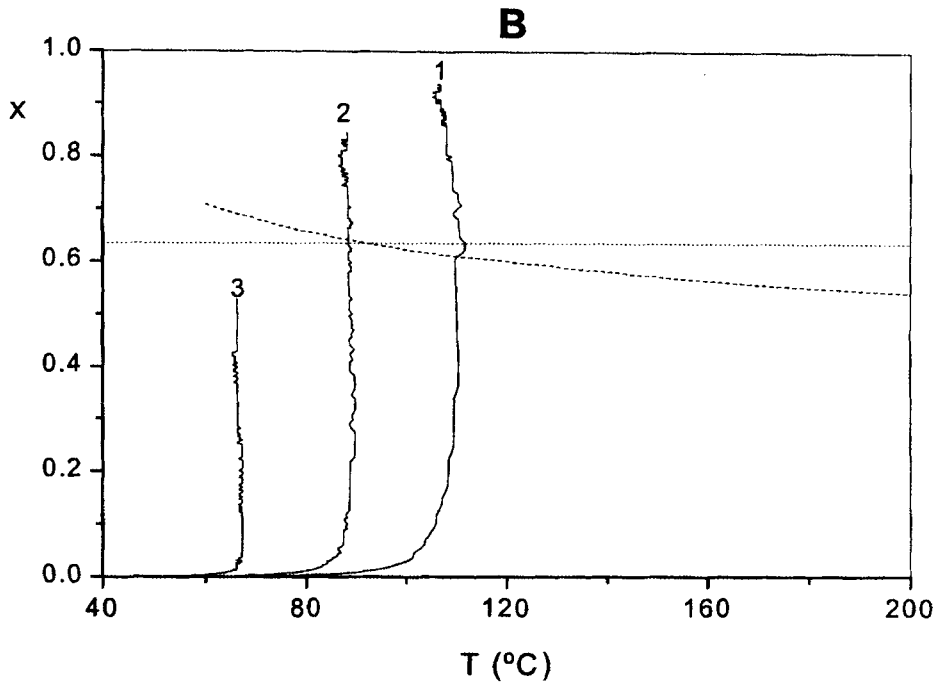

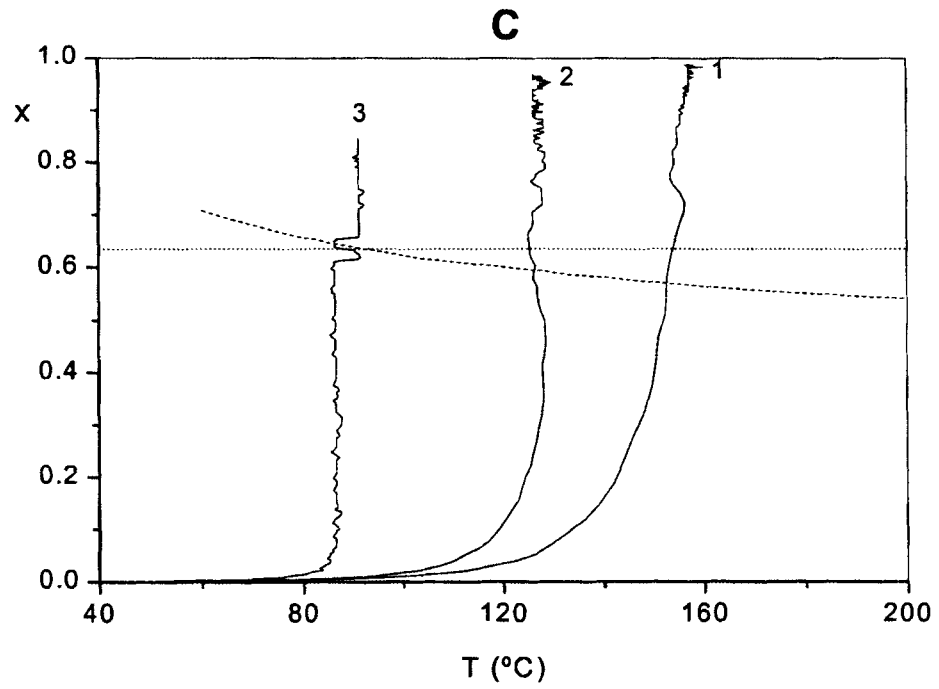

Fig. 4. Continued.

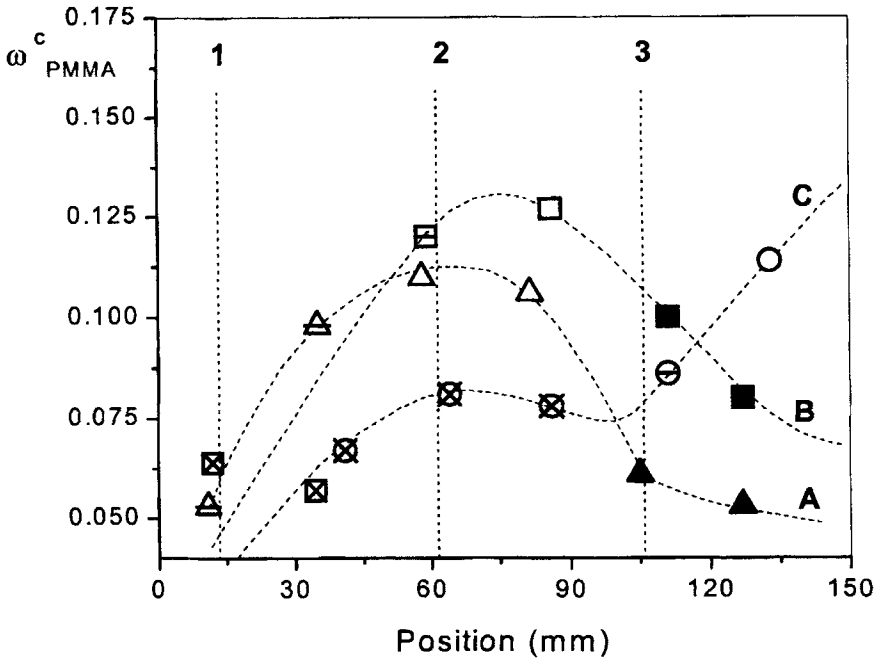

Fig. 5. Mass fraction of PMMA dissolved in the matrix, ω^c_{PMMA}, vs. position along the mold, for each temperature profile; A: (△), B: (□) and C: (○). Open symbols correspond to transparent sections, dot center symbols correspond to translucent sections and the corresponding opaque sections are represented by X center symbols or solid ones depending if the separation process occurs during cure or postcure time, respectively.

are represented by X center symbols or solid ones depending upon whether the separation process occurs during cure or postcure time, respectively. For transparent samples the remaining mass fraction of PMMA dissolved in the matrix is higher than 0.1.

Figure 6 shows the morphology gradient for the sample obtained with profile B through TEM and AFM images, corresponding to positions 1, 2 and 3; morphologies of intermediate positions are only shown with AFM images. The appearance of AFM sequence (opaque, translucent or transparent) agrees with Fox equation results shown on *Fig. 5*. The micrographs corresponding to positions 1 and 3, opaque samples, show rows of spherical domains like brain circumvolutions; while the micrograph corresponding to position 2, the translucent sample, shows very small particles. Domain size distribution of sample at position 1, phase separated during cure at lower temperature, is narrower than that of the sample at position 3, phase separated during postcure at higher temperature.

Figure 7 shows AFM images of samples obtained with A, B, and C profiles at positions 1, 2 and 3. Images for A1, B2 and C3 have a similar morphology with small domains and consequently they are translucent. On the other hand, it is clearly observed that opaque images for B1, C1, and C2 (phase separated during the cure) and for A3 and B3 (phase separated during the postcure) have grater domains. The image for A2 shows a transparent aspect because at this point the system gels without phase separation. These results agree with x-T trajectories followed during the cure (see *Figs. 4a, 4b*, and *4c*) and with mass fractions of PMMA dissolved in the matrix calculated with the Fox equation (see *Fig. 5*).

CONCLUSIONS

The miscibility of the modifier used in this study decreases with cure temperature and the cloud point of the modified system is close to the gel point of the matrix. If polymer gelates at temperatures lower than 91.5°C, the material will be transparent, with lower glass transition and therefore higher mass fraction of PMMA dissolved in the matrix.

The size and the position of the transparent zone depend on temperature profile and curing time. Therefore, it becomes possible to change properties along a material with an unique chemical formulation by controlling only the processing conditions.

From the viewpoint of practical applications, these experimental results not only provide insight into manufacturing polymeric materials with variable gradients of structure (i.e. gradients of properties), but also, if the aim of the modifier addition is to obtain a material with uniform properties, the cure must be carefully considered.

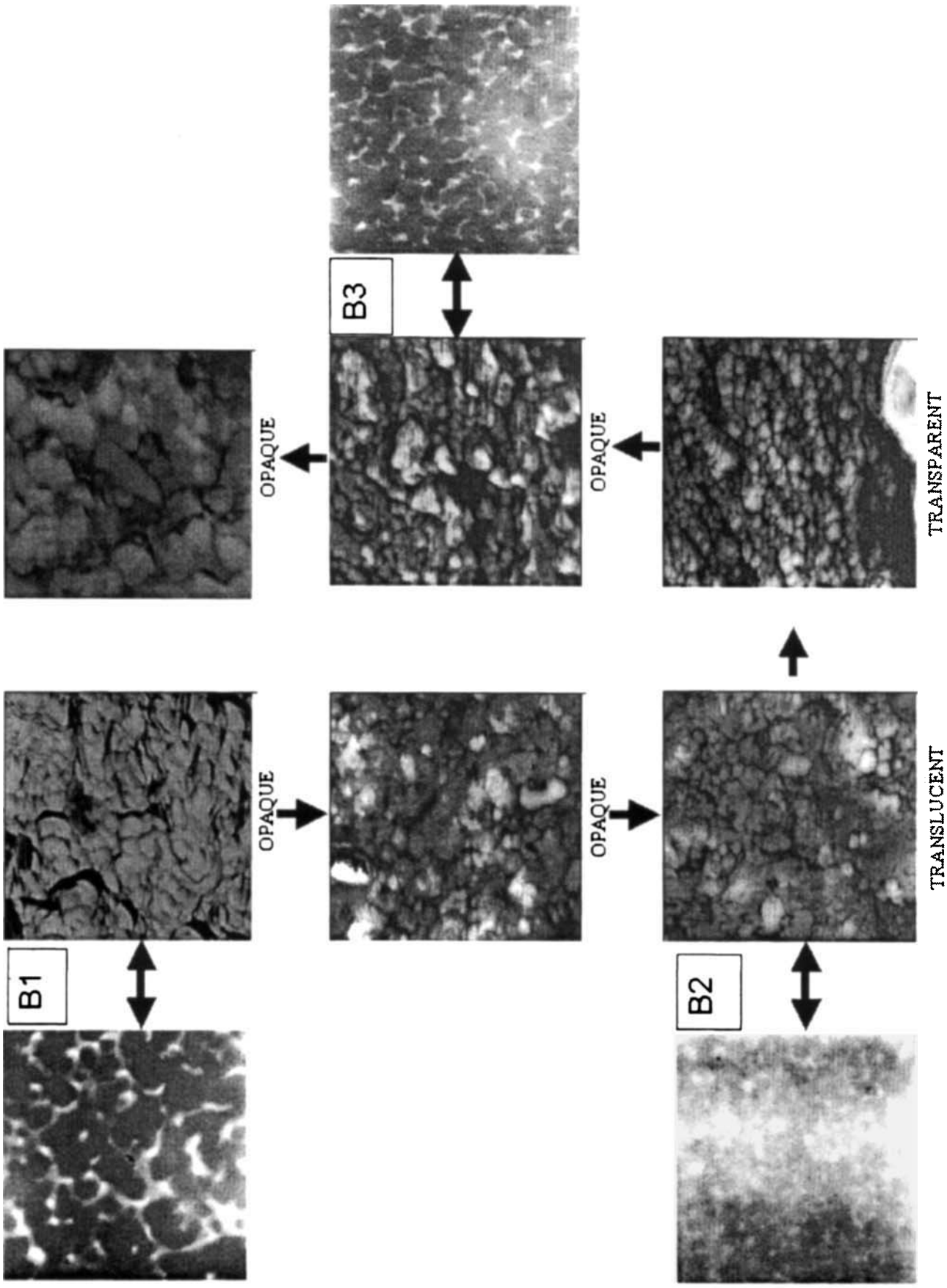

Fig. 6. Arrows connect the sequence of six AFM images (phase image) obtained in tapping mode of postcure sample processed with profile B. Double arrows relate AFM micrographs obtained at positions 1, 2 and 3 with the corresponding TEM images.

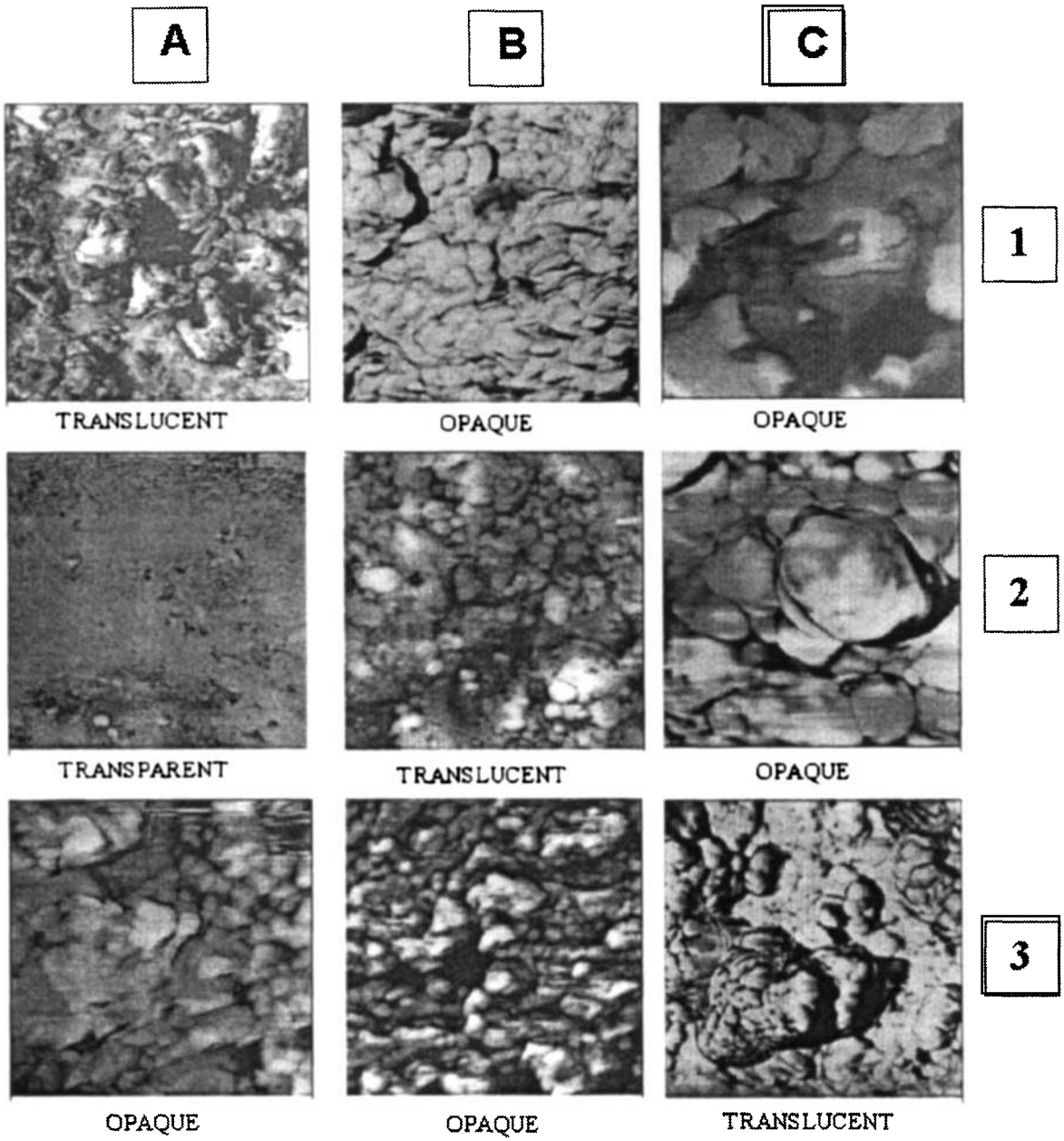

Fig. 7. AFM image (phase image) for the profiles A, B and C for the positions 1, 2 and 3.

REFERENCES

1. B. J. Cardwell and A. F. Yee, *Polymer*, **34**, 1695 (1993).
2. B. Geisler and F. N. Kelley, *J. Appl. Polym. Sci.*, **54**, 177 (1994).
3. H. J. Sue, J. L. Bertram, E. I. Garcia Meitin, and P. M. Puckett, *J. Polym. Sci.: Part B: Polym. Phys.*, **33**, 2003 (1995).
4. J. Kinloch, S. J. Shaw, D. A. Tod, and D. L. Hunston, *Polymer*, **24**, 1341 (1983).
5. F. Yee and R. A. Pearson, *J. Mater. Sci.*, **21**, 2462 (1986).
6. B. Bucknall and I. K. Partridge, *Polym. Eng. Sci.*, **26**, 54 (1986).
7. J. L. Hedrick, I. Yilgor, M. J. Jurek, J. C. Hedrick, G. L. Wilkens, and J. E. McGrath, *Polymer*, **32**, 2020 (1991).
8. T. Iijima, H. Hiraoka, and M. Tomoi, *J. Appl. Polym. Sci.*, **45**, 709 (1992).
9. F. Meyer, G. Sanz, A. Eceiza, I. Mondragón, and J. Mijovic, *Polymer*, **36**, 1407 (1995).
10. P. Huang, S. Zheng, J. Huang, Q. Guo, and W. Zhu, *Polymer*, **38**, 5565 (1997).
11. P. A. Oyanguren, C. C. Riccardi, R. J. J. Williams, and I. Mondragón, *J. Polym. Sci. Part B: Polym. Phys. Ed.*, **36**, 1349–1359 (1998).
12. C. C. Riccardi, J. Borrajo, R. J. J. Williams, E. Girard-Reydet, H. Sautereau, and J. P. Pascault, *J. Polym. Sci., B: Polym. Phys.*, **34**, 349 (1996).
13. D. Verchère, H. Sautereau, J. P. Pascault, S. M. Moschiar, C. C. Riccardi, and R. J. J. Williams, in *Toughened Plastics I: Science and Engineering*, p. 355, C. K. Riew and A. J. Kinloch, eds., Washington D.C. (1993).
14. C. C. Riccardi, J. Borrajo, and R. J. J. Williams, *Polymer*, **35**, 5541 (1994).

15. J. B. Holt, M. Koizumi, T. Hirai, and Z. A. Munir, *Cer. Trans.*, **34**, 3 (1993).
16. D. Pu.Fang, P. M. Frontini, C. C. Riccardi, and R. J. J. Williams, *Polym. Eng. Sci.*, **35**, 1359 (1995).
17. C. B. Bucknall, G. Maïstros, C. M. Gómez, and I. K. Partridge, *Makromol. Chem. Macromol. Symp.*, **70/71**, 255 (1993).
18. D. S. Porter and T. C. Ward, "Characterization and mechanical properties of gradient temperature cure toughened policianuratos," 20th annual meeting of ACS, Carolina del Sur (1997).
19. H. Nishioka, K. Kida, O. Yano, and Q. Tran-Cong, *Macromolecules*, **33**, 4301 (2000).
20. I. Mondragón, P. M. Remiro, M. D. Martin, A. Valea, M. Franco, and V. Bellenguer, *Polym. Intern.*, **47**, 152 (1998).
21. P. M. Remiro, C. C. Riccardi, M. A. Corcuera, and I. Mondragón , *J. Appl. Polym. Sci.*, **74**, 772 (1999).
22. P. M. Remiro, C. C. Riccardi, and I. Mondragón, "Design of Mechanical Behaviour in PMMA-modified epoxy resins by control of phase separation," 216th ACS National meeting, Boston (August 1998).
23. H. J. Choi, M. S. Cho, C. A. Kim, and M. S. Jhon, *Polym. Eng. Sci.*, **39**, 1473 (1999).
24. C. C. Riccardi and A. Vazquez, *Polym. Eng. Sci.*, **29**, 120 (1989).
25. J. Mijovic and H. T. Wang, *SAMPE J.*, March/April, 42 (1988).
26. S. Sourour and M. R. Kamal, *Polym. Eng. Sci.*, **16**, 480 (1976).
27. T. G. Fox, *Bull. Am. Phys. Soc.*, **1**, 123 (1956).